ORIGINAL ARTICLE

Thermal imaging of increment cores: a new method to estimate sapwood depth in trees

Malkin Gerchow[1] · John D. Marshall[2] · Kathrin Kühnhammer[1,3] · Maren Dubbert[4] · Matthias Beyer[1]

Abstract

The cells in tree sapwood form a network of interconnected conduits which enables the transport of water and nutrients from the tree roots to the canopy. Sapwood depth must be assessed when tree water use is estimated from sap flow velocities. However, current approaches to assess sapwood depth are either not applicable universally, or require expensive instruments, the application of chemicals or laborious field efforts. Here, we present a new method, which estimates sapwood depth by thermal imaging of increment cores. Using a low-cost thermal camera for mobile devices, we show that the sapwood–heartwood boundary is detectable by a sharp increase in temperature. Estimated sapwood depths agree with dye estimates ($R^2 = 0.84$). We tested our approach on a broad range of temperate and tropical tree species: *Quercus robur, Pinus sylvestris, Swietenia macrophylla*, *Guazuma ulmifolia*, *Hymenaea courbaril*, *Sideroxylon capiri* and *Astronium graveolens.* In nearly all species, the methods agreed within 0.6 cm. Thermal imaging of increment cores provides a straightforward, low-cost, easy-to-use, and species-independent tool to identify sapwood depth. It has further potential to reveal radial differences in sapwood conductivity, to improve water balance estimations on larger scales and to quickly develop allometric relationships.

Keywords Thermal imaging · Sapwood depth · Increment core · Sapwood conductivity

Introduction

The cells within sapwood form a network of interconnected conduits that engage in the transport of water and nutrients from the tree roots to the canopy. Sapwood also acts as a water and carbohydrate storage until its cells die and transform into heartwood. Not all parts of the sapwood must be conductive, in many species only the outermost sapwood

engages in the transport of water. Hence, sapwood should be further classified into conductive sapwood (i.e., wood still able to transport water) and storage sapwood (i.e., wood having mainly storage functions) (Lehnebach et al. 2018). In this study, we define sapwood as the conductive wood of the tree. The assessment of sapwood depth is of importance for many applications in forestry, plant physiology and hydrology.

For example, the most established methods to quantify the amount of water transpired by trees are based on heat dissipation. Sensor needles are inserted at discrete points into the sapwood to relate heat dissipation to sap flow velocities (Granier 1987; Marshall 1958; Smith and Allen 1996). For estimating whole tree water use, sap flow velocities must be integrated over the sapwood area, which requires an accurate estimation of sapwood depth. Much work has been done to improve the sap flow estimates, e.g., by reducing the influence of sapwood wounding (Burgess et al. 2001; Green et al. 2008; Vandegehuchte and Steppe 2012), by adaptation to different plant sizes (Clearwater et al. 2009; Hanssens et al. 2013) and by covering wider ranges of sap flow velocities (Forster 2019). However, upscaling of measured velocities remains difficult. Small errors in sapwood depth estimations

✉ Malkin Gerchow
  m.gerchow@tu-bs.de

1 Institute for Geoecology, Technische Universität Braunschweig, Langer Kamp 19c, 38106 Brunswick, Germany

2 Department of Forest Ecology and Management, Swedish University of Agricultural Sciences, Umeå, Sweden

3 Chair of Ecosystem Physiology, University of Freiburg, Georges-Köhler-Allee 53, 79110 Freiburg, Germany

4 Leibniz Center for Agricultural Landscape Research (ZALF), Isotope Biogeochemistry and Gas Fluxes, Müncheberg, Germany

accumulate during the upscaling process, i.e., upscaling flow velocities to water use of a single tree, single tree water use to a stand and stand water use to the catchment or ecosystem scale. Another challenging aspect of upscaling is radial variation in sap flow velocities (Ford et al. 2007; Oishi et al. 2008). Such radial variation exists because only a part of the sapwood might engage in the transport of fluid. Specifically, sap flow velocities decrease from the outer part to the inner part of the sapwood in many species. Therefore, ideally radial sap flow profiles are considered when sapflow velocities are integrated (Caylor and Dragoni 2009; Reyes-Acosta and Lubczynski 2014; Zhang et al. 2015), as scaling up point estimates of sap flow velocities based on a dichotomization of conductive and non-conductive wood is known to lead to bias in water use estimates (Berdanier et al. 2016; Reyes-Acosta and Lubczynski 2013).
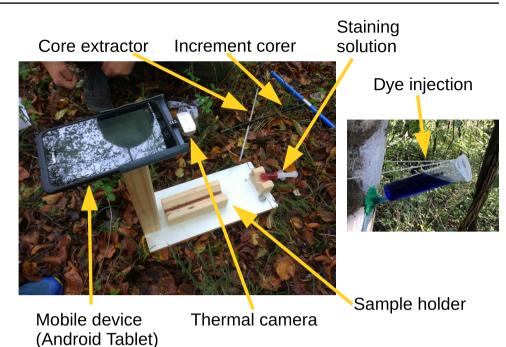
If sapwood depth is successfully determined, it can be used to infer important canopy parameters such as leaf area or biomass (McDowell et al. 2002; van der Sande et al. 2015). The sapwood–heartwood boundary is also of importance when analyzing differences in nutrient concentrations, chemical composition and morphology (Bertaud and Holmbom 2004). Both sapwood (Gartner and Meinzer 2005; Pineda-García et al. 2013) and heartwood (Hu et al. 2018) have been shown to release water to maintain transpiration under dry conditions. Hence, to understand their individual contribution to the total stem water storage a distinction between sap- and heartwood is required.

Several methods have been developed to estimate sapwood depth by locating the sapwood–heartwood boundary. Most commonly increment cores are visually inspected and interpreted based on experience or stained before assessment (to improve sapwood visibility) and the boundary is directly inferred (Wang et al. 2010; Pfautsch et al. 2011; Nakada et al. 2019). However, separation of sapwood from heartwood by visual inspection is not possible for all species (Hoadley 1990) and is subjective, at best. Staining requires a different indicator solution for each species, but suitable solutions are known only for well-studied species (Kutscha and Sachs 1962). Another approach is to inject dye into the conductive stream, i.e., a hole for the injection is drilled into the trunk before an increment core is taken above the injection point. Sapwood can then be identified from the presence of dye on the core. However, additional drilling for the injection point further damages the tree and high transpiration is required for the dye uptake (Gebauer et al. 2008; Gotsch et al. 2010; Brantley et al. 2016). When sapwood vessels transform into heartwood, they become increasingly obstructed and the hydraulic conductivity decreases in some species (Holbrook and Zwieniecki 2005). In this way, identification of the sapwood depth by incident light microscopy is sometimes possible (Pfautsch et al. 2010; Pfautsch 2016). Sapwood depth can potentially be estimated from radial sap

flow profiles (Molina et al. 2016). Other approaches utilize advanced technologies. X-ray computed tomography (CT) can detect changes in densities and moisture content (Danvind and Ekevad 2006; Fromm et al. 2001). Similar properties can be measured with electric resistivity tomography (ERT) (Bieker and Rust 2010; Guyot et al. 2013; Wang et al. 2016; Benson et al. 2019). Both approaches require expensive instruments and are inaccessible for most users. Additionally, moisture content is not necessarily different between sapwood and heartwood (Pfautsch and Macfarlane 2016). Near-infrared spectroscopy (NIR) detects changes in chemical composition of materials and can be used to separate sapwood from heartwood, but requires an extensive model calibration for each target species (Pfautsch et al. 2012). Little effort has been invested into developing methods based on thermal imaging.

In this case, the water stored in the xylem starts to evaporate when exposed to unsaturated air. When a water molecule near the surface absorbs enough energy to overcome the vapor pressure, it will evaporate into the surrounding air as a gas. The energy removed by the vaporized molecule will reduce the temperature of the water and hence cool down the surface. Following this physical law, varying rates of evaporation between sapwood and heartwood would produce a temperature difference. The magnitude of evaporative cooling mostly depends on the relative humidity of the surrounding air (vapor pressure), the temperature of the water (kinetic energy of the molecules), and the amount of water and surface area available for evaporation. In many species, especially conifers, the water content is higher within sapwood compared to heartwood. The temperature difference might be detected by a thermal camera. This approach was first described in a semi-industrial application by analyzing thermal images of crosscut pine saw logs (Gjerdrum and Høibø 2004). Differences in water content are often less pronounced for hardwood species (Peck 1959). Therefore, a difference at the sapwood–heartwood boundary in the evaporation rate and consequently a change in temperature can be caused by either a difference in moisture content or by a change of hydraulic conductivity. The hydraulic conductivity of trees decreases towards the heartwood due to the formation of tyloses and gum deposition (Lehnebach et al. 2018). We, therefore, hypothesize that the location of the highest temperature gradient occurs at the sapwood–heartwood boundary.

In this study, we developed a new method to determine sapwood depth based on thermal infrared imaging of tree increment cores. Therefore, we used an uncooled thermal sensor developed for mobile devices. These cameras are inexpensive (ca. 200–500 USD), easily deployable (can be attached directly to a smartphone) and are receiving increasing attention in the scientific community (García-Tejero et al. 2018; Petrie et al. 2019; Noguera et al. 2020).

Fig. 1 Experimental setup; low-cost thermal camera, mobile device, sample holder, increment corer, dyeing solution and dye injection

Core extractor   Increment corer   Staining solution

Dye injection

Mobile device (Android Tablet)   Thermal camera   Sample holder

Our objectives are to (i) test if a temperature difference across increment cores is detectable with a low-cost thermal camera, (ii) propose an objective procedure to calculate a sapwood–heartwood boundary based on the detected temperature difference, (iii) analyze if the detected sapwood–heartwood boundary is comparable to a boundary determined by staining and dye injection and (iv) evaluate the applicability of our method on a range of temperate and tropical species, i.e., English oak (*Q. robur*), Scots pine (*P. sylvestris),* Caoba (*S. macrophylla*), Guacimo (*G. ulmifolia),* Guapinol (*H. courbaril*), Tempisque (*S. capiri)* and Ronron (*A. graveolens).*

Materials and methods

Study areas and sampling

Increment cores were taken at two sites; a humid temperate forest and a tropical dry forest. For each studied site, a random selection of healthy, mature trees was sampled. In total, seven species were investigated. *Quercus robur* and *P. sylvestris* were sampled in mid-October 2019 around Hannover, Lower Saxony, Germany (52° 18′ 56″ N, 9° 35′ 09″ E, 63°m a.s.l.). The tropical dry forest species *S. macrophylla, G. ulmifolia, H. courbaril, S. capiri* and *A. graveolens* were sampled in June 2021 during the wet season (first rain event in April, leaf unfurling in May) near Liberia, Guanacaste, Costa Rica (10° 42′ 46″ N, 85° 35′ 46″ W, 100°m a.s.l.). Sapwood depths estimated by our method were validated against increment core staining and dye injection. The European

species were dyed by staining the cores with an indicator solution and the sapwood–heartwood boundary was inferred afterwards by visual assessment. Tropical dry forest species were dyed by injecting dye into the conductive stream as no applicable dyeing solution for these species was known. In total, 32 increment cores originating from seven different species were evaluated.

Increment cores (5.15 mm diameter) were taken at breast height (1.3 m) with an increment borer (10-100-1031, Haglöf Sweden 2018). On average the cores had a length of 9.4 cm, the smallest being 2.4 cm and the largest 14.2 cm. Immediately after extracting the increment core, it was placed into a bag without removing the core from the extractor. The sample removal from the trunk was done in way to preserve wood structure orientation, i.e., the surface that included open vessels within the sapwood pointed towards the camera. After 10 min the sample was placed in a custom-made core holder (Fig. 1) that was placed 35 cm below a thermal camera (TE-M1, I3-System 2019). The time between sample removal and thermal imaging allowed the dissipation of heat introduced by the coring process, i.e., for homogenizing the increment core. The camera was focused once on the increment core and a calibration step was applied for each sample, i.e., flat field correction (FFC) was performed by closing the lens with a cap and the FFC procedure was executed in the camera's mobile app. Subsequently, a thermal image of the sample was taken every 3 s over a period of 1 min. For the tropical dry forest species, a second set of images with increased evaporation rate was taken. Preliminary studies showed no detectable temperature difference between sapwood and heartwood without artificially

increasing evaporation. Therefore, to increase evaporation, samples were exposed to a cold and hot air stream from a hairdryer. To ensure a uniform air stream on the sample the stream was applied from a distance of ca. 1 m with a small waving motion. Thermal images were taken during and after the air stream every 3 s for 1 min. The total recording time for one sample took about 5 min.

A second increment core was taken to analyze the effect of the moisture content profile on our method; the second core was required as cores were exposed to evaporation for up to 5 min. Each core was sliced into 20 mm sections. For each section, the fresh and dry weight (oven dried for 48 h at 100 °C) was determined. The water content in percent was calculated as the difference between fresh and dry weight, divided by dry weight.

Increment core staining and dye injection

Sapwood depths estimated by our method were validated against two established methods; Increment core staining and dye injection. Whenever possible increment core staining was chosen as it is straightforward if staining solutions for the target species are known. In case that no applicable staining solution was found (tropical dry forest species) dye injection was chosen.

Each sample of *Q. robur* and *P. sylvestris* was visually inspected after thermal images were recorded. A methyl orange solution was applied to the *Q. robur* samples; it produced contrasting colors between sapwood and heartwood due to difference in pH (Kutscha and Sachs 1962).

Tropical dry forest species were dyed by injecting dye (Brilliantblau FCF, C.I. No. 42090, Omikron, Germany) into the conductive stream below the sampling point, following (Gebauer et al. 2008). For this, a sunny day was chosen to ensure high transpiration rates and therefore high sapflow velocities to reach a sufficient dye transport. In the morning (7 AM) a hole (diameter 3.5 mm, depth 7.5 cm) was drilled into the tree trunk at a slight angle 2 cm below breast height. Immediately after the drilling, dye was injected into the hole with a syringe applying slight pressure until excess dye started to leak. Afterwards a syringe was attached to the hole and additional dye was injected every 30 min for the next 3 h. After 6 h increment cores were taken 2 cm above the injection point. The dyed sapwood–heartwood boundary was visually determined by noting the position at which no more dye was visible on the core (Fig. 2a).

Thermal image processing

Thermal images were directly saved on the connected mobile device in the Comma-Separated Values (CSV) format. Each cell in the tabular file represented one pixel of the thermal image (240×180 pixel); it contained the measured

temperature value in degrees Celsius. All recorded files were loaded and further processed with a custom tool[1] written in Python 3.9 (Python Core Team 2019). A median filter with a kernel size of 3 pixels was applied over all images to reduce sensor noise and all pixels across the center of the increment core were extracted using bilinear interpolation from the thermal images. This resulted in a temperature profile across the length of the core.
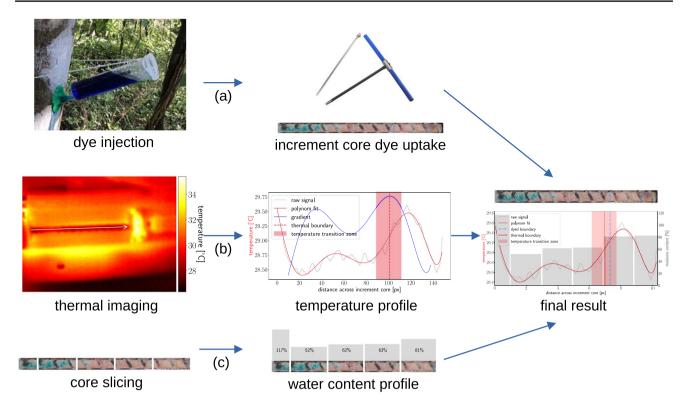
Sapwood–heartwood boundary detection based on thermal imaging

Similar to previous work using ERT (Benson et al. 2019; Guyot et al. 2013; Wang et al. 2016), a polynomial regression was fitted to the data points of each extracted temperature profile. The fitted polynomial with the highest R^2 value was then used to determine the location of the global maximum in the temperature gradient. On average, a polynomial of degree 8 was fitted to 130 temperature observations (i.e., average increment core length in pixel). Border effects at the transition to ambient temperature of 1 cm at the beginning and end of the temperature profile were not considered.

The transformation from sapwood to heartwood occurs gradually, therefore a locally precise sapwood–heartwood boundary may not exist. We used the sharpness of the temperature increase to define a temperature transition zone, i.e., the section were the temperature increases from a lower temperature (assumedly sapwood temperature) to higher temperature (assumedly heartwood temperature). The temperature transition zone is defined as the continuous temperature increase around the maximum of the temperature gradient, over which the temperature gradient does not fall below 85% of its relative maximum value (Fig. 2b) and was calculated by the function peak_widths from the scipy.signal package (Virtanen et al. 2020). The relative height was chosen iteratively such that the transition zone spans over the temperature increase at the detected sapwood–heartwood boundary for all samples.

Linear regression analysis between dyed and thermal sapwood boundaries was done with statsmodels 0.13.2 (Seabold and Perktold 2010). We used the following metrics to compare the overall agreement between thermal imaging and dyeing methods: the coefficient of determination R^2 to describe random deviations from the linear regression (Fig. 4a), the mean signed difference and the mean absolute difference to describe systematic deviations (Table 1). Systematic deviations and the limit of agreement was further

---

[1] The tool to analyze thermal images of increment cores is available under https://git.rz.tu-bs.de/m.gerchow/thermal-imaging-increment-cores

Fig. 2 Study workflow; **a** dye is either injected into the tree trunk (dry forest species) or the core is stained by an indicator solution (European species). The sapwood–heartwood boundary is estimated by visual assessment of dye coloring on the increment core. **b** The temperature profile is extracted across the increment core (i.e., along the white arrow) from the thermal image. The sapwood–heartwood boundary is estimated by locating the global maximum in the temperature gradient (vertical red dashed line). **c** A second increment core is sliced into small sections. The water content profile is determined from the fresh and dry weight of each section. The final result consists of the increment core temperature profile (red line), the sapwood–heartwood boundary determined by thermal imaging (vertical red dashed line) and by dyeing (vertical blue dashed line), the temperature transition zone (light red) and the cores water content profile (light blue)

analyzed in a Bland–Altman plot (Bland and Altman 1986) (Fig. 4b).

Results

Dye injection and staining

Separation of sapwood and heartwood was possible in 30 of 32 tested cores using dye injection (tropical species) and staining (European species). In two cores (*S. capiri*) either no dye was present on the core or dye was present until the pith (Fig. 3d, f). Samples from other species showed a varying degree of dye uptake. While cores of *G. ulmifolia* and *S. capiri* displayed a high amount of dye uptake, *H. courbaril* and *A. graveolens* cores showed a lower and discontinuous dye uptake, i.e., dotted pattern including gaps (Fig. 3). Only one of the tropical species (*S. macrophylla*) showed a visible color difference between sapwood and heartwood, i.e., all other species required a dedicated method to separate sapwood from heartwood. The bright-colored sapwood in

S. macrophylla was the only section where injected dye was present and subsequently was identified as sapwood (Fig. 3a–c). The sapwood of *P. sylvestris* was distinguishable without staining (Fig. 3p, q, f). *Quercus robur* showed a distinctive reddish colored heartwood compared to an orange-colored sapwood after staining (Fig. 3s–u). Across all species and tree sizes, the average estimated sapwood depth was 3.5 ± 2.0 cm (mean $\pm$ standard deviation) while the smallest sapwood depth was 2.0 ± 0.5 cm (*H. courbaril*) and the largest was 6.1 ± 2.0 cm (*S. capiri*) (Table 1).
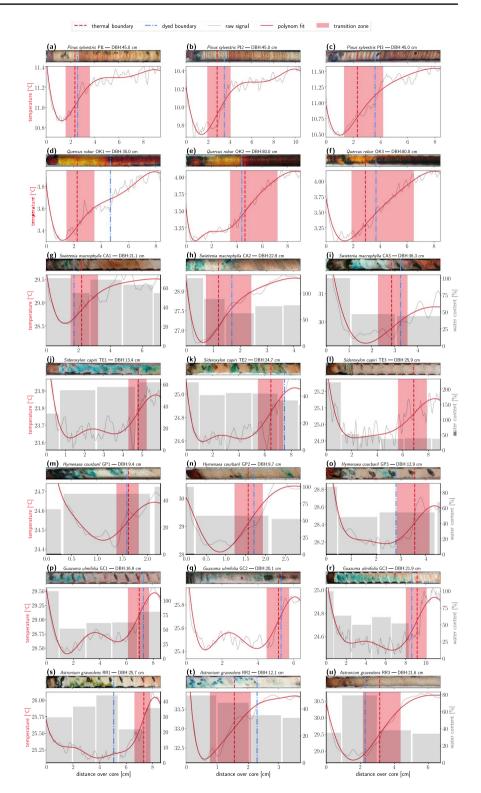
Thermal imaging

We detected a prominent temperature increase (i.e., peak in the gradient of the fitted polynomial) in all analyzed temperature profiles. On average the temperature at the peak increased 0.5 ± 0.5 °C/cm while *S. capiri* (0.2 ± 0.1 °C/cm), *Q. robur* (0.2 ± 0.0 °C/cm) and *P. sylvestris* (0.2 ± 0.1 °C/cm) showed a lower increase compared to a higher increase in *G. ulmifolia* (0.8 ± 0.8 °C/cm) and *A. graveolens* (0.8 ± 0.5 °C/cm) (Table 1).

Table 1 Summary statistics of thermal imaging and dyed sapwood–heartwood boundaries for each species

Species	No. dyed / thermal imaged	Tree diameter range [cm]	Dyed sapwood boundary [cm]	Thermal sapwood boundary [cm]	Mean signed difference [cm]	Mean absolute difference [cm]	Dyed boundary within temperature transition zone	Temperature gradient at thermal boundary [°C/cm]	Temperature difference between sapwood and heartwood [°C]	Sapwood area difference [%]	Mean water content [%]
Swietenia macrophylla	6/6	14.3–36.3	2.7±1.0	2.5±0.9	0.2±0.5	0.4±0.3	5/6	0.5±0.3	0.6±0.4	2.7±18.7	63.0±11.0
Guazuma ulmifolia	6/6	16.2–21.9	4.3±3.2	4.5±3.2	−0.1±0.4	0.3±0.2	5/6	0.8±0.8	0.7±0.6	−10.6±18.6	64.0±9.0
Hymenaea courbaril	4/4	9.4–12.9	2.0±0.5	2.1±1.0	−0.0±0.5	0.4±0.3	2/4	0.8±0.9	0.5±0.6	2.3±16.3	52.0±6.0
Quercus robur	3/3	35.0–80.0	4.3±0.5	3.3±1.2	1.0±1.4	1.2±1.1	2/3	0.2±0.0	0.6±0.3	20.9±26.6	–
Pinus sylvestris	3/3	45.0–45.0	3.2±0.6	2.5±0.3	0.7±0.5	0.7±0.5	3/3	0.2±0.1	0.5±0.2	19.8±13.1	–
Astronium graveolens	6/6	7.3–25.7	3.5±1.8	4.0±2.3	−0.5±1.0	0.8±0.8	2/6	0.8±0.5	0.7±0.5	−8.9±22.1	39.0±8.0
Sideroxylon capiri	2/4	13.4–25.9	6.1±2.0	5.5±1.5	1.0±0.0	1.0±0.0	0/2	0.2±0.1	0.2±0.1	11.4±4.0	48.0±9.0
Total	30/32	7.32–80.0	3.5±2.0	3.5±2.1	0.2±0.8	0.6±0.6	19/30	0.5±0.5	0.6±0.4	2.2±20.6	53.3±11.6

Values are displayed as mean ± standard deviation

Fig. 3 Temperature profiles of increment cores taken by thermal imaging. Three examples are shown for each of the seven analyzed species. A polynomial (red line) was fitted to the raw temperature signal (gray line). The sapwood–heartwood boundary was determined by dyeing and thermal imaging. The thermal boundary (vertical red dashed line) was detected by locating the highest temperature increase in the temperature profile. The zone of the temperature increase is highlighted in light red. The dyed boundary (vertical blue dotted dashed line) was determined by locating the point at which no more dye is present on the increment core. For each tropical dry forest species an increment core was sliced into sections to determine a water content profile (gray bars)
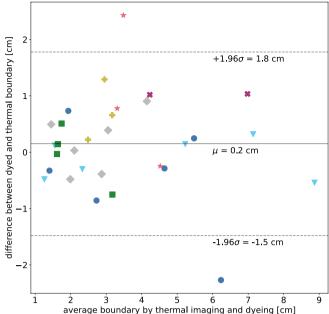

Estimated sapwood sections by dyeing corresponded to a local minimum in temperature (Fig. 3). *S. capiri* and *G. ulmifolia* showed slight temperature variations elsewhere in the sapwood as well (Fig. 3). On average, the detected sapwood section over all species was 0.6 ± 0.4 °C colder than the heartwood. *G. ulmifolia* and *A. graveolens*

showed the highest temperature difference between heartwood and sapwood (0.7 ± 0.6 and 0.7 ± 0.5 °C) and *S. capiri* the lowest (0.2 ± 0.1 °C) (Table 1).

Fig. 4 Comparison of sapwood–heartwood boundaries detected by dyeing and thermal imaging. In total 30 increment cores over seven different species were compared. The thermal boundary was detected by locating the highest temperature increase in the temperature across the increment core. The dyed boundary was determined by either injecting dye into the conductive stream (dry forest species) or by staining cores with a dyeing solution (European species). Thermal imaging of increment cores is a statistically significant predictor of dyed sapwood depths ($t(28) = 11.89$, $p < 0.001$). The linear regression model explained 84% of the variances within dyed sapwood depths and is statistically significant ($R^2 = 0.84$, $F(1, 28) = 141.3$, $p < 0.001$)
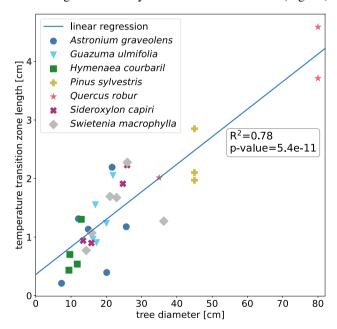
Increment core water content analysis

No obvious change in water content was detected at the dyed sapwood–heartwood boundaries (Fig. 3). On average over all samples the water content was $53.3 \pm 11.6\%$. *S. macrophylla* and *G. ulmifolia* had the highest water content ($63.0 \pm 11.0\%$ and $64.0 \pm 9.0\%$) compared to the lowest water content in *A. graveolens* ($39.0 \pm 8.0\%$) (Table 1).

Comparison of thermal and dyed estimated sapwood depths

Sapwood–heartwood boundaries detected by our method were comparable to the dyed boundaries ($R^2 = 0.84$; Fig. 4). The boundary depth estimates fell nearly on the 1:1 line (Fig. 4a). On average the difference between the dyed sapwood depth and thermal detected was 0.2 ± 0.8 cm with an absolute difference of 0.6 ± 0.6 cm over all analyzed cores (Fig. 4; Table 1). Absolute differences between both methods were lower than 0.5 cm for *S. macrophylla* (0.4 ± 0.3 cm), *G. ulmifolia* (0.3 ± 0.2 cm) and *H. courbaril* (0.4 ± 0.3 cm) and 1 cm for *Q. robur* (1.2 ± 1.1 cm) and *S. capiri* (1.0 ± 0.0 cm) (Table 1). The highest absolute difference (> 2 cm) between the two methods was reached by a *Q. robur* (2.4 cm) (Fig. 3d) and a *A. graveolens* (-2.3 cm) (Fig. 3s); both these samples lay outside of the 95% confidence interval (Fig. 4b).

Limit of agreement analysis between both methods (Fig. 4b)

Fig. 5 Relationship of tree diameter and the length of the temperature transition zone. The temperature transition zone is defined as the temperature gradient peak width, in which the temperature increases from a lower sapwood temperature to higher heartwood temperature. The length of the transition zone significantly increased with increasing tree diameter ($t(29) = 10.09$, $p < 0.001$)

indicated that dyed sapwood depths may be underestimated by 1.5 cm (lower 95% confidence interval) or overestimated by 1.8 cm (upper 95% confidence interval) when compared to sapwood depths detected by thermal imaging. In 19 out of 30 samples the dyed sapwood–heartwood boundary was within the temperature transition zone (Table 1). Sapwood areas calculated from validated sapwood depths were 20% greater for *Q. robur* ($20.9 \pm 26.6\%$) and *P. sylvestris* ($19.8 \pm 13.1\%$) and 10% less for *G. ulmifolia* ($-10.6 \pm 18.6\%$) and *A. graveolens* ($-8.9 \pm 22.1\%$) when compared to areas calculated from thermal sapwood depths. On average over all samples the sapwood area differed by $2.2 \pm 20.6\%$ (Table 1). The length of the temperature transition zone (i.e., sharpness of the temperature increase at the thermal boundary) increased with tree diameter independently of the species ($R^2 = 0.74$; Fig. 5).

Discussion

In this study, we developed and tested a novel method to estimate the sapwood depth of trees using thermal imaging of increment cores. Analyzed temperature profiles showed a clearly detectable temperature increase at the sapwood–heartwood boundary, i.e., a significant positive peak in the temperature gradient at the boundary of sap- and heartwood. We speculate that this sharp change in temperature is associated with a sharp decrease in hydraulic conductivity of the wood.

A comparison between dyed- and thermal boundaries revealed a very good agreement for the seven investigated species. Estimated sapwood depths agreed with dye estimates ($R^2 = 0.84$; Fig. 4). The average absolute difference across all species was 0.61 cm (Table 1). Absolute differences between both methods were lower than 0.5 cm for *S. macrophylla*, *G. ulmifolia* and *H. courbaril* and 1 cm for *Q. robur* and *S. capiri*. On average sapwood areas calculated from dyed- and thermal boundaries only differ by 2%. Sapwood areas of *P. sylvestris* and *Q. robur* calculated from thermal boundaries were around 20% smaller. ERT measurements show similar systematic deviation of sapwood depths by staining solutions in *P. sylvestris* (Bieker and Rust 2010). In the case of *Q. robur* temperature variations within the sapwood can cause large difference between the sapwood depth detected by dyeing and thermal imaging (Fig. 3d). *Quercus robur* is known to carry 95% of its water in the two outermost annual rings (Cermák et al. 1992), which potentially caused the detected temperature variation within the sapwood. At the other extreme, we detected a temperature increase which clearly indicated a sapwood–heartwood boundary but a change in dye coloring was not present (Fig. 3l). Dye injection methods require transport of dye away from the injection point to stain the increment core

taken above the injection point. In environmental condition with low transpiration rates and therefore low sap flow the uptake of dye can be limited (Brantley et al. 2016). We observed similar effects in preliminary tests where in some cases no dye uptake took place or only an insufficient coloring was present.

A perfect agreement between both methods over a wide range of species is unlikely as an exact boundary between sapwood and heartwood does not exist in general. Instead, the process of transforming sapwood into heartwood happens gradually and ends with the death of parenchyma cells (Bamber 1976). Similar, the conductivity of sapwood progressively declines inward until it completely ceases when it transforms into heartwood (Pfautsch 2016). This decline in conductivity was also revealed by injecting dye in the conductive stream, i.e., a stronger dye uptake was present at the outermost sapwood for *H. courbaril* and *G. ulmifolia* (Fig. 3). In contrast, visual assessment of increment cores (with or without staining) does not necessarily correspond to the conductive sapwood, especially for ring-porous species (Lehnebach et al. 2018).

The width of the temperature transition zone increased with increasing tree diameter ($R^2 = 0.74$; Fig. 5). Similarly, the sap flow profile of tropical dry forest species is known to be dependent on the tree size (Link et al. 2020). In a future study, a potential relationship between the transition zone (or in general the temperature profile of increment cores) and the sap flow profile should be analyzed.

Other methodologies to assess sapwood depth (ERT, CT), depend on a gradient in moisture content between sapwood and heartwood. However, this requirement is not met for all species, e.g., Eucalyptus (Pfautsch et al. 2012) and other hardwood species (Peck 1959). Our results show a similar pattern as no consistent difference in moisture content between sapwood and heartwood was present in any of the analyzed tropical dry forest species. Nevertheless, a temperature difference between sapwood and heartwood was still detectable by thermal imaging. We argue that increment cores in which sapwood and heartwood have equal moisture content still can create a temperature gradient as a higher conductive sapwood can supply water to the evaporating surface more quickly than the less conductive heartwood.

While a sapwood–heartwood separation based on thermal images was previously demonstrated (Gjerdrum and Høibø 2004), we have extended the application to multiple species and used increment cores instead of crosscut logs. This opens up the possibility for an easy to use and general applicable method for sapwood depth detection. Further studies should analyze the environment effects on the method as the tropical dry forest samples (relative humidity > 90%) required an artificial increase in evaporation to strengthen the temperature signal. This was done using a standard hairdryer while other means are certainly possible, e.g., briefly

heating increment cores in an oven before imaging or using air-conditioned rooms during imaging.

The possibility to rapidly detect the conductive sapwood will enable researchers to improve water balance estimations on larger scales. In future work, a potential relationship between radial sap flow profiles and temperature profiles derived from thermal images of increment cores should be investigated.

Declarations

Conflict of interest The authors have no relevant financial or non-financial interests to disclose.

References

Bamber RK (1976) Heartwood, its function and formation. Wood Sci Technol 10(1):1–8. https://doi.org/10.1007/BF00376379

Benson AR, Koeser AK, Morgenroth J (2019) Estimating conductive sapwood area in diffuse and ring porous trees with electronic resistance tomography. Tree Physiol 39(3):484–494. https://doi.org/10.1093/treephys/tpy092

Berdanier AB, Miniat CF, Clark JS (2016) Predictive models for radial sap flux variation in coniferous, diffuse-porous and ring-porous temperate trees. Tree Physiol 36(8):932–941. https://doi.org/10.1093/treephys/tpw027

Bertaud F, Holmbom B (2004) Chemical composition of earlywood and latewood in Norway spruce heartwood, sapwood and transition zone wood. Wood Sci Technol 38(4):245–256

Bieker D, Rust S (2010) Non-destructive estimation of sapwood and heartwood width in Scots pine (*Pinus sylvestris* L.). Silv Fenn 44(2):267–273

Bland JM, Altman DG (1986) Statistical methods for assessing agreement between two methods of clinical measurement. Lancet (london, England) 1(8476):307–310

Brantley ST, Schulte ML, Bolstad PV, Miniat CF (2016) Equations for estimating biomass, foliage area, and sapwood of small trees in the Southern Appalachians. For Sci 62(4):414–421

Burgess SSO, Adams MA, Turner NC, Beverly CR, Ong CK, Khan AAH, Bleby TM (2001) An improved heat pulse method to measure low and reverse rates of sap flow in woody plants. Tree Physiol 21(9):589–598. https://doi.org/10.1093/treephys/21.9.589

Caylor KK, Dragoni D (2009) Decoupling structural and environmental determinants of sap velocity: part I methodological development. Agric for Meteorol 149(3–4):559–569

Cermák J, Cienciala E, Kucera J, Hällgren JE (1992) Radial velocity profiles of water flow in trunks of Norway spruce and oak and the response of spruce to severing. Tree Physiol 10(4):367–380. https://doi.org/10.1093/treephys/10.4.367

Clearwater MJ, Luo Z, Mazzeo M, Dichio B (2009) An external heat pulse method for measurement of sap flow through fruit pedicels, leaf petioles and other small-diameter stems. Plant Cell Environ 32(12):1652–1663

Danvind J, Ekevad M (2006) Local water vapor diffusion coefficient when drying Norway spruce sapwood. J Wood Sci 52(3):195–201

Ford CR, Hubbard RM, Kloeppel BD, Vose JM (2007) A comparison of sap flux-based evapotranspiration estimates with catchment-scale water balance. Agric for Meteorol 145(3–4):176–185

Forster M (2019) The dual method approach (DMA) resolves measurement range limitations of heat pulse velocity sap flow sensors. Forests 10(1):46. https://doi.org/10.3390/f10010046

Fromm JH, Sautter I, Matthies D, Kremer J, Schumacher P, Ganter C (2001) Xylem water content and wood density in spruce and oak trees detected by high-resolution computed tomography. Plant Physiol 127(2):416–425

García-Tejero IF, Ortega-Arévalo CJ, Iglesias-Contreras M, Moreno JM, Souza L, Tavira SC, Durán-Zuazo VH (2018) Assessing the crop-water status in almond (*Prunus dulcis* Mill.) trees via thermal imaging camera connected to smartphone. Sensors 18(4):1050

Gartner BL, Meinzer FC (2005) 15 - Structure-function relationships in sapwood water transport and storage. Vasc Transp Plant 2005:307–331. https://doi.org/10.1016/B978-012088457-5/50017-4

Gebauer T, Horna V, Leuschner C (2008) Variability in radial sap flux density patterns and sapwood area among seven co-occurring temperate broad-leaved tree species. Tree Physiol 28(12):1821–1830

Gjerdrum P, Høibø O (2004) Heartwood detection in Scots pine by means of heat-sensitive infrared images. Holz Als Roh-Und Werkst 62(2):131–136

Gotsch SG, Geiger EL, Franco AC, Goldstein G, Meinzer FC, Hoffmann WA (2010) Allocation to leaf area and sapwood area affects water relations of co-occurring savanna and forest trees. Oecologia 163(2):291–301. https://doi.org/10.1007/s00442-009-1543-2

Granier A (1987) Evaluation of transpiration in a Douglas-fir stand by means of sap flow measurements. Tree Physiol 3(4):309–320

Green S, Clothier B, Perie E (2008) A re-analysis of heat pulse theory across a wide range of sap flows. VII Int Workshop Sap Flow 846:95–104

Guyot A, Ostergaard KT, Lenkopane M, Fan J, Lockington DA (2013) Using electrical resistivity tomography to differentiate sapwood from heartwood: application to conifers. Tree Physiol 33(2):187–194. https://doi.org/10.1093/treephys/tps128

Hanssens J, De Swaef T, Nadezhdina N, Steppe K (2013) Measurement of sap flow dynamics through the tomato peduncle using a

non-invasive sensor based on the heat field deformation method. IX Int Workshop Sap Flow 991:409–416

Hoadley RB (1990) Identifying wood: accurate results with simple tools. Taunton Press, New Town

Holbrook NM, Zwieniecki MA (2005) Vascular transport in plants. Elsevier Academic Press, Cambridge. https://doi.org/10.1016/B978-0-12-088457-5.X5000-X

Hu G, Liu H, Shangguan H, Wu X, Xu X, Williams M (2018) The role of heartwood water storage for semi-arid trees under drought. Agric for Meteorol 256–257:534–541. https://doi.org/10.1016/j.agrformet.2018.04.007

Kutscha NP, Sachs IB (1962) Color tests for differentiating heartwood and sapwood in certain softwood tree species (Report 2246). United States Department of Agriculture and Forest Service, Madison WI, USA

Lehnebach R, Beyer R, Letort V, Heuret P (2018) The pipe model theory half a century on: a review. Ann Bot 121(5):773–795

Link RM, Fuchs S, Arias Aguilar D, Leuschner C, Castillo Ugalde M, Valverde Otarola JC, Schuldt B (2020) Tree height predicts the shape of radial sap flow profiles of Costa-Rican tropical dry forest tree species. Agric for Meteorol 287:107913

Marshall DC (1958) Measurement of sap flow in conifers by heat transport. Plant Physiol 33(6):385

McDowell N, Barnard H, Bond B, Hinckley T, Hubbard R, Ishii H, Köstner B, Magnani F, Marshall J, Meinzer F (2002) The relationship between tree height and leaf area: sapwood area ratio. Oecologia 132(1):12–20

Molina AJ, Aranda X, Carta G, Llorens P, Romero R, Savé R, Biel C (2016) Effect of irrigation on sap flux density variability and water use estimate in cherry (*Prunus avium*) for timber production: azimuthal profile, radial profile and sapwood estimation. Agric Water Manag 164:118–126. https://doi.org/10.1016/j.agwat.2015.08.019

Nakada R, Okada N, Nakai T, Kuroda K, Nagai S (2019) Water potential gradient between sapwood and heartwood as a driving force in water accumulation in wetwood in conifers. Wood Sci Technol 53(2):407–424

Noguera M, Millán B, Pérez-Paredes JJ, Ponce JM, Aquino A, Andújar JM (2020) A new low-cost device based on thermal infrared sensors for olive tree canopy temperature measurement and water status monitoring. Remote Sens 12(4):723

Oishi AC, Oren R, Stoy PC (2008) Estimating components of forest evapotranspiration: a footprint approach for scaling sap flux measurements. Agric for Meteorol 148(11):1719–1732

Peck EC (1959) The sap or moisture in wood. Report. United States Forest Products Laboratory, (R768)

Petrie PR, Wang Y, Liu S, Lam S, Whitty MA, Skewes MA (2019) The accuracy and utility of a low cost thermal camera and smartphone-based system to assess grapevine water status. Biosyst Eng 179:126–139

Pfautsch S (2016) Hydraulic anatomy and function of trees—basics and critical developments. Curr for Rep. https://doi.org/10.1007/s40725-016-0046-8

Pfautsch S, Macfarlane C (2016) Comment on Wang et al. quantifying sapwood width for three Australian native species using electrical resistivity tomography. Ecohydrology 9(5):894–895

Pfautsch S, Bleby T, Rennenberg H, Adams M (2010) Sap flow measurements reveal influence of temperature and stand structure on water use of *Eucalyptus regnans* forests. For Ecol Manag 259:1190–1199. https://doi.org/10.1016/j.foreco.2010.01.006

Pfautsch S, Keitel C, Turnbull TL, Braimbridge MJ, Wright TE, Simpson RR, O'Brien JA, Adams MA (2011) Diurnal patterns of water use in *Eucalyptus victrix* indicate pronounced desiccation–rehydration cycles despite unlimited water supply. Tree Physiol 31(10):1041–1051. https://doi.org/10.1093/treephys/tpr082

Pfautsch S, Macfarlane C, Ebdon N, Meder R (2012) Assessing sapwood depth and wood properties in *Eucalyptus* and *Corymbia* spp. Using visual methods and near infrared spectroscopy (NIR). Trees 26(3):963–974

Pineda-García F, Paz H, Meinzer FC (2013) Drought resistance in early and late secondary successional species from a tropical dry forest: the interplay between xylem resistance to embolism, sapwood water storage and leaf shedding. Plant Cell Environ 36(2):405–418. https://doi.org/10.1111/j.1365-3040.2012.02582.x

Python Core Team (2019) Python: a dynamic, open source programming language. Python Software Foundation. https://www.python.org/. Accessed 3 Apr 2021

Reyes-Acosta JL, Lubczynski MW (2013) Mapping dry-season tree transpiration of an oak woodland at the catchment scale, using object-attributes derived from satellite imagery and sap flow measurements. Agric for Meteorol 174:184–201

Reyes-Acosta JL, Lubczynski MW (2014) Optimization of dry-season sap flow measurements in an oak semi-arid open woodland in Spain. Ecohydrology 7(2):258–277

Seabold S, Perktold J (2010) statsmodels: Econometric and statistical modeling with python. In: Proceedings of the 9th Python in Science Conference

Smith DM, Allen SJ (1996) Measurement of sap flow in plant stems. J Exp Bot 47(12):1833–1844

van der Sande MT, Zuidema PA, Sterck F (2015) Explaining biomass growth of tropical canopy trees: the importance of sapwood. Oecologia 177(4):1145–1155. https://doi.org/10.1007/s00442-015-3220-y

Vandegehuchte MW, Steppe K (2012) Sapflow+: a four-needle heat-pulse sap flow sensor enabling nonempirical sap flux density and water content measurements. New Phytol 196(1):306–317. https://doi.org/10.1111/j.1469-8137.2012.04237.x

Virtanen P, Gommers R, Oliphant TE, Haberland M, Reddy T, Cournapeau D, Burovski E, Peterson P, Weckesser W, Bright J (2020) SciPy 1.0: fundamental algorithms for scientific computing in Python. Nat Method 17(3):261–272

Wang Y-L, Liu G-B, Kume T, Otsuki K, Yamanaka N, Du S (2010) Estimating water use of a black locust plantation by the thermal dissipation probe method in the semiarid region of Loess Plateau, China. J for Res 15(4):241–251

Wang H, Guan H, Guyot A, Simmons CT, Lockington DA (2016) Quantifying sapwood width for three Australian native species using electrical resistivity tomography. Ecohydrology 9(1):83–92

Zhang J-G, He Q-Y, Shi W-Y, Otsuki K, Yamanaka N, Du S (2015) Radial variations in xylem sap flow and their effect on whole-tree water use estimates. Hydrol Process 29(24):4993–5002